CHINESE OPTICS LETTERS

Vol. 20, No. 9 | September 2022

Investigations on beam quality improvement of an NCPM-KTA-based high energy optical parametric oscillator using an unstable resonator with a Gaussian reflectivity mirror [Invited]

Jun Meng (孟 君)[1], Chen Li (李 晨)[1], Zhenhua Cong (丛振华)[1,2,3], Zhigang Zhao (赵智刚)[1,2,3], Shang Wang (王 上)[3], Gaoyou Liu (刘高佑)[2,3,4], and Zhaojun Liu (刘兆军)[1,2,3*]

[1] School of Information Science and Engineering, Shandong University, Qingdao 266237, China

[2] Shandong Provincial Key Laboratory of Laser Technology and Application, Qingdao 266237, China

[3] Key Laboratory of Laser & Infrared System (Shandong University), Ministry of Education, Qingdao 266237, China

[4] Center for Optics Research and Engineering, Shandong University, Qingdao 266237, China

*Corresponding author: zhaojunliu@sdu.edu.cn

Received April 4, 2022 | Accepted May 13, 2022 | Posted Online June 13, 2022

Beam quality improvements by a large margin for signal and idler beams of a high energy 100 Hz $KTiOAsO_4$ (KTA) non-critical phase matching (NCPM) optical parametric oscillator (OPO) were demonstrated using an unstable resonator configuration instead of a plane-parallel one. Theoretically, influences of cavity lengths and transmission of an output coupler on the OPO conversion efficiency for both were numerically simulated. For OPO based on an unstable resonator with a Gaussian reflectivity mirror, the maximum pulse energies at the signal (1.53 μm) and idler (3.47 μm) were about 75 mJ and 26 mJ, respectively. The corresponding beam quality factors of the signal were $M_x^2 = 9.8$ and $M_y^2 = 9.9$, and $M_x^2 = 11.2$ and $M_y^2 = 11.5$ for the idler. As a comparison, 128 mJ of signal and 48 mJ of idler were obtained with the plane-parallel resonator, and the M^2 factors of the signal were $M_x^2 = 39.8$ and $M_y^2 = 38.4$, and $M_x^2 = 32.1$ and $M_y^2 = 31.4$ for the idler. Compared with a plane-parallel cavity, over eight times and three times brightness improvements were realized for the signal and idler light, respectively.

Keywords: optical parametric oscillators; unstable resonator; beam quality.
DOI: 10.3788/COL202220.091401

1. Introduction

Optical parametric oscillators (OPOs)[1] are able to effectively generate high energy lasers at the eye-safe (1.5 μm)[2,3] and mid-infrared (MIR, 3–5 μm) wavelengths, which are located in atmospheric transmission windows, and thus are widely used in remote sensing, spectroscopy, and countermeasures[4,5]. Usually, nonlinear crystals, for example, $KTiOPO_4$ (KTP), $ZnGeP_2$ (ZGP), $KTiOAsO_4$ (KTA) are adopted. KTP crystals exhibit strong absorption in the MIR band with an absorption peak at 3.4 μm, resulting in low MIR energy output[6,7]. For ZGP crystals, 2 μm pumping sources are needed[8–10], whereas a 1 μm pump source is more mature and readily available in high energy sources with high repetition rate. Comparatively speaking, KTA crystals show high damage threshold (≥600 MW/cm^2), large nonlinear coefficient ($d_{24} = 3.2$ pm/V), and large acceptance angle[11,12], which were widely used in high energy short-wave and middle-wave infrared sources[13].

Except for pulse energy, beam quality is another concern for distance-related applications. In fact, simple plane-parallel cavities are widely used for high energy nanosecond pulsed OPOs[14,15]; however, the beam qualities are not so satisfactory. For example, in 2001, McCarthy *et al.* reported a KTP-OPO system with a pulse repetition frequency (PRF) of 10 Hz, in which a pulse energy of 123 mJ at 1.57 μm was achieved with a beam quality factor (M^2) of 23[16]. In 2010, Liu *et al.* obtained 151 mJ signal (1.5 μm) and 53 mJ idler (3.6 μm) by a plane-parallel cavity OPO at 10 Hz PRF, in which the divergence angle of the idler was 34 mrad without mentioning beam quality[17]. Recently, we also reported a plane-parallel cavity-based KTA-OPO system with a PRF of 100 Hz, and the total (signal + idler) pulse energy was 242 mJ. However, the M^2 factor was measured to be about 30[18].

To improve the beam quality of high energy OPO systems, there are mainly two methods, one of which is the non-planar

ring cavity configuration, including the rotated image singly resonant twisted rectangle (RISTRA)[19] and fractional image rotation enhancement (FIRE)[20] resonator. In 2021, Medina *et al.* demonstrated beam quality improvement for a 10 kHz ZGP-OPO system with both non-planar ring resonators (M^2~1.8 in RISTRA and $M^2 \sim 1.4$ in FIRE). However, the total (signal + idler) pulse energy was only 2.1 mJ at 3–5 μm, even if the average power reached 21 W[21]. In 2004, Armstrong demonstrated an *xz*-cut KTA-based OPO with a RISTRA cavity to generate 1.55 μm light with $M^2 \sim 4$, where the PRF was 10 Hz with an average power of 1.5 W[22]. To date, non-planar ring cavities are mostly used in ZGP-OPO, while high energy KTA-OPOs are rarely reported because the improvement in beam quality comes from the combined effect of image rotation and birefringent walk-off in the nonlinear crystal. Therefore, these configurations are not suitable for non-critical phase matching (NCPM) crystals-based OPO systems[23]. NCPM can maximize the acceptance angle and effective nonlinear coefficient of nonlinear crystals. KTA-OPO with NCPM has a large acceptance angle, which greatly reduces the requirements for the beam quality of the pump light, while eliminating the walk-off effect to maximize the effective gain length[24].

Another well-established method for brightness improvement is to employ unstable resonators, which are simple in structure[25] and can lead to enhancement of brightness with acceptable energy loss[26,27]. The unstable resonator can be classified as a uniform mirror (URM) or non-URM (NURM) by the radial profile of output mirror reflectivity[28]. Both theories[29] and experiments[30,31] have proved that URM unstable resonators can be used to generate high energy lasers with high beam quality in OPOs. In 1998, Scharpf *et al.* reported a URM unstable cavity eye-safe OPO with a pulse energy of 82 mJ at 50 Hz PRF, whose beam quality was measured to be about 4.7 times diffraction limited[32]. In 2001, Hansson *et al.* reported a $RbTiOAsO_4$ OPO with a URM unstable resonator, where the M^2 factors of the signal at 1.56 μm and idler at 3.33 μm were about 7 and 2.5, respectively. However, the total pulse energy was only 5 mJ at 10 Hz PRF[33]. In 2006, Vodchits *et al.* obtained a pulse energy of 22 mJ at 1.578 μm with 2 Hz PRF by a URM unstable cavity OPO, in which the divergence angle was 3.5 mrad without mentioning beam quality[34]. However, the URM unstable resonators usually show a high threshold due to high loss, and the ring-shaped output beam contains a diffraction ring with a hot spot at the center, which limits the development of OPOs with unstable resonators. The unstable resonator based on a Gaussian reflectivity mirror (GRM) can eliminate these shortcomings[35–38]. Therefore, the unstable cavity OPO based on a GRM has attracted tremendous research interest[39]. To the best of our knowledge, thus far, a 100-mJ-level OPO laser system with an unstable resonator at 100 Hz PRF has not been reported. We are encouraged to combine the NCPM KTA crystal and GRM unstable cavity to explore how the brightness could be improved with simple but robust configurations.

In this contribution, we compared the performances of two OPO cavities, i.e., stable plane-parallel resonator and unstable resonator. A total output energy of 170 mJ was obtained in the plane-parallel cavity, where the M^2 factors for the signal were $M_x^2 = 39.8$ and $M_y^2 = 38.4$, and $M_x^2 = 32.1$ and $M_y^2 = 31.4$ for the idler. Based on theoretical calculations and experimental results, the parameters of the resonator were optimized and improved, and the unstable cavity based on a GRM was designed, which greatly improved the beam quality. A total output energy of 101 mJ was obtained, with the M^2 factors of $M_x^2 = 9.8$ and $M_y^2 = 9.9$ for the signal and $M_x^2 = 11.2$ and $M_y^2 = 11.5$ for the idler. Compared with the plane-parallel cavity, the brightness of the signal and idler was improved by more than eight times and three times, respectively. The experimental results show that the unstable cavity with GRM is more suitable for high brightness OPOs based on NCPM-KTA.

2. Numerical Simulation

The parametric interaction of OPOs can be described by the coupled field equations[40]:

$$\frac{\partial E_s(x,y,z)}{\partial z} = i\frac{\omega_s}{cn_s} d_{\text{eff}} E_p(x,y,z) E_i^*(x,y,z) e^{i\Delta kz} + \frac{i}{2k_s}(\nabla_x^2 + \nabla_y^2) E_s(x,y,z), \tag{1a}$$

$$\frac{\partial E_i(x,y,z)}{\partial z} = i\frac{\omega_i}{cn_i} d_{\text{eff}} E_p(x,y,z) E_s^*(x,y,z) e^{i\Delta kz} + \frac{i}{2k_i}(\nabla_x^2 + \nabla_y^2) E_i(x,y,z), \tag{1b}$$

$$\frac{\partial E_p(x,y,z)}{\partial z} = i\frac{\omega_p}{cn_p} d_{\text{eff}} E_s(x,y,z) E_i(x,y,z) e^{-i\Delta kz} + \frac{i}{2k_p}(\nabla_x^2 + \nabla_y^2) E_s(x,y,z), \tag{1c}$$

where E_s, E_i, and E_p are the amplitudes of the signal, idler, and pump fields with the angular frequencies ω_s, ω_i, and ω_p, respectively. Here, it is assumed that the phase match condition can be satisfied, $\Delta k = 0$. The term d_{eff} denotes the effective nonlinear coefficient. n_s, n_i, and n_p are the refractive indices of the crystal for the signal, idler, and pump waves, respectively. c is the speed of light in vacuum, and the direction of light propagation follows the z axis.

The pump power follows a Gaussian time distribution given by

$$P_p = \frac{2\sqrt{\ln 2}W_p}{\sqrt{\pi}\tau} e^{-\left(\frac{2\sqrt{\ln 2}t}{\tau}\right)^2}, \tag{2}$$

where W_p is the single-pulse energy of the pump wave, and τ is the pulse width of the pump wave.

Also, the transverse distribution of the intensity is assumed to be Gaussian, and it is given by

$$I = \frac{2P_p}{\pi\omega_{0,p}^2} e^{-\frac{2(x^2+y^2)}{\omega_{0,p}^2}}, \tag{3}$$

where $\omega_{0,p}$ represents the beam radius.

Using $I = 1/2(nc\varepsilon_0 E^2)$ and assuming that the beam waist is located at the input mirror, one can obtain the temporal and spatial profile of the pump pulse, given by

$$E_p = \left(\frac{8\sqrt{\ln 2}}{n_p c\varepsilon_0 \pi\omega_{0,p}^2\sqrt{\pi}\tau}\right)^{\frac{1}{2}} e^{-\frac{(x^2+y^2)}{\omega_{0,p}^2}} e^{-2\left(\frac{\sqrt{\ln 2}t}{\tau}\right)^2}. \tag{4}$$

The initial intensity of the signal wave is the vacuum fluctuations, given by Ref. [41],

$$I_{so} = \frac{\hbar\omega_s}{\pi\omega_{0,s}^2\tau_s}, \tag{5}$$

which plays a key role in starting the parametric oscillation. τ_s is the round trip time, and $\omega_{0,s}$ is the beam radius of the resonating signal wave.

The evolution of three waves can be simulated as follows, the process of which is similar to Ref. [42]. The pump pulse is injected on the crystal surface and experiences the energy conversion due to the nonlinear frequency conversion inside the nonlinear crystal. Then, the reflected waves by the output mirror become the start values of the next cavity round trip. Also, this loop will end after the pump pulse leaves the crystal.

Note that a Gaussian mirror is used in the unstable cavity OPO, whose transmission exhibits a Gaussian profile,

$$T(r) = T_{\max} e^{-\frac{2r^2}{\omega_m^2}}, \tag{6}$$

where ω_m is the mirror radius, and $T_{\max}$ is the central transmittance of the mirror.

The calculation results are the spatial and temporal distribution of the electrical field of three waves. Subsequently, one can get the output energy of three waves using the integration, given by

$$W_q = \int_{-\infty}^{\infty} dt \iint_{-\infty}^{\infty} \frac{1}{2} n_q c\varepsilon_0 |E_q|^2 dx dy, \qquad q = s, i. \tag{7}$$

The conversion efficiency of the OPO can also be calculated from the relation

$$\eta = \frac{W_s + W_i}{W_{in}}, \tag{8}$$

where W_s *and* W_i are the single-pulse energy of the signal and idler wave.

Conversion efficiency is a key factor to decide the optimum OPO, and it has attracted much interest to improve the conversion efficiency recently[43]. Parameters of the OPO can be easily optimized based on the numerical simulation, which may help the experiment operation. For the simulation, the nonlinear coefficient d_{eff} is taken as 3.2 pm/V. The pump, signal, and idler wavelengths are $\lambda_s = 1535$ nm, $\lambda_p = 1064$ nm, and $\lambda_i = 3467$ nm, respectively. The refractive indices are $n_s = 1.776$, $n_p = 1.868$, and $n_i = 1.74$. Firstly, the dependence of the conversion efficiency on the crystal length was evaluated, as shown in Fig. 1(a). The shorter crystal length led to a lower conversion efficiency due to the incomplete conversion, and the conversion efficiency reaches a maximum around the 30 mm length. It indicated that a suitable crystal length can be used to optimize the OPO, and it may be about 30–35 mm for our experimental arrangement.

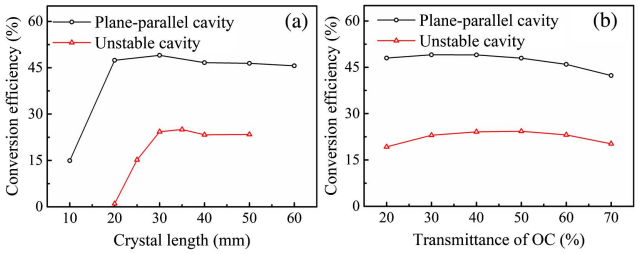

Fig. 1. (a) Conversion efficiency versus crystal length at 50% transmittance of the OC. (b) Conversion efficiency versus transmittance of the OC at the crystal length of 33 mm.

The efficiency of the plane-parallel cavity is approximately twice that of the unstable cavity, mainly due to the fact that the output coupler (OC) of the plane-parallel cavity is high reflection (HR) coated at 1.064 μm, whereas the OC of the unstable cavity is not. The influence of the mirror transmittance on the conversion efficiency was also analyzed, as shown in Fig. 1(b). Based on our simulations, the optimum value of the transmittance was predicted to be around 45% for our experiment. The numerical model is beneficial to optimize OPO parameters.

3. Experimental Setup

The experimental setup of the high energy KTA OPO system is depicted in Fig. 2. The system was composed of 1064 nm $Nd:Y_3Al_5O_{12}$ (Nd:YAG) main oscillator power amplifier (MOPA) and KTA-OPO. The side-pumped Nd:YAG MOPA system contained an oscillator and two-stage amplifiers, which were used as the pump source of the KTA-OPO.

In the Nd:YAG MOPA system, the master oscillator was designed to operate at a PRF of 100 Hz *Q*-switched by an electro-optic modulator (EOM). To compensate for the thermally induced birefringence, the double-rods-cascading structure was adopted, and a 90° quartz rotator was placed between the two rods. The oscillator consisted of two 0.6% (atomic fraction) Nd:YAG rods with a diameter of 5 mm and a length of 75 mm, which were placed in a resonator with a length of 35 cm. GRM1 was the OC with 30% reflectivity at 1.064 μm, which could improve the beam quality of the oscillator. The peak pump power of the single module used in the oscillator, first-stage amplifier, and second-stage amplifier was 3 kW, 6 kW,

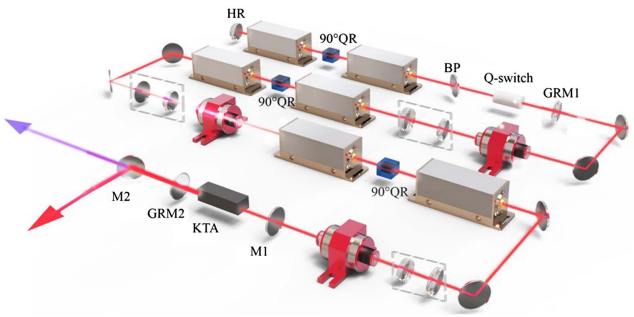

Fig. 2. Schematic diagram of the experimental setup of the KTA-OPO system. HR, high reflection; 90°QR, 90° quartz rotator; BP, beam polarizer; GRM1, Gaussian reflectivity mirror for 1.06 μm; ISO, isolator; M1, mirror 1; GRM2, Gaussian reflectivity mirror for 1.5 μm; M2, 45° beam splitter.

and 12 kW, respectively. Isolators were placed between the amplifier stages to prevent self-excited oscillation and amplified spontaneous emission between the amplifiers, which could also protect the optical components from damage. The Nd:YAG rods of the first and second-stage amplifiers were 0.6% doped with sizes of $\Phi 6 \times 130$ mm and $\Phi 7 \times 188$ mm, respectively.

According to the simulation results, an X-cut KTA crystal was used as the nonlinear crystal with a size of 10 mm × 10 mm × 33 mm. The Nd:YAG MOPA system was used as the pump source of the OPO, which was injected into the OPO cavity through the isolator and the collimation system. To make a comparison, plane-parallel and unstable resonators were designed under the same experimental conditions. The input mirror of the OPO (M1) was coated with high transparency (HT) for pump light and HR for signal and idler light. Both the OCs of stable and unstable cavities were coated with a reflectivity of 50% for the signal and HT for the idler. The OC of the plane-parallel cavity was coated with HR for the 1.064 μm wavelength, while GRM2 of the unstable cavity was not. As explained in Ref. [29], for the unstable cavity, the cavity losses were directly related to the magnification factor m, which should be a good trade-off between the round-trip losses and the spatial mode selection. Through experimental optimization, GRM2 and the rearview mirror were finally selected to form a non-confocal unstable cavity with $m = 1.49$. The M1 was a concave mirror with a radius of 2000 mm, and GRM2 was a Gaussian reflectivity convex mirror with a radius of 1300 mm. In the stable resonator, cavity mirrors were both flat mirrors.

4. Results and Discussion

4.1. The 1064 nm pump source

The output energy of the Nd:YAG oscillator, first-stage amplifier, and second-stage amplifier is shown in Fig. 3. The maximum output pulse energy of the pump source was about 480 mJ. The typical pulse shape at the maximum output energy of the Nd:YAG MOPA system is shown in Fig. 3(a), and the pulse duration of the final output laser was about 18 ns. As

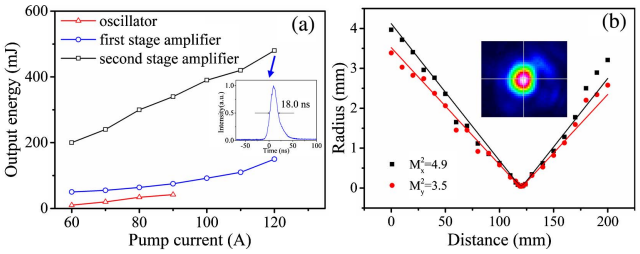

Fig. 3. (a) Output energy change with the pump current. Inset shows the temporal pulse profile at maximum output power. (b) Beam quality of the energy at 480 mJ. Inset shows the beam profile.

shown in Fig. 3(b), M_x^2 and M_y^2 for 480 mJ output energy were 4.9 and 3.5, respectively. The inset in Fig. 3(b) shows the corresponding transverse beam profile. For an introduction to the 1064 nm pump source, refer to Ref. [16] for specific results.

4.2. The KTA-OPO

A beam expander system was applied to match the pump beam diameter with the crystal aperture. The diameter of the pump laser injected into the KTA-OPO was 8 mm. The crystal was wrapped with indium foil and mounted in a crystal holder. To compare the output characteristics of unstable and stable cavities, both were demonstrated with the same cavity length of 90 mm. The corresponding pulse energies of the OPO versus the pump energy are shown in Fig. 4(a). When the maximum incident pump energy was 480 mJ, the total output energy of the unstable resonator with GRM was 101 mJ, of which the 1.53 μm signal light was 75 mJ, and the 3.47 μm idler light was 26 mJ. The highest total output energy of the plane-parallel cavity was 170 mJ with the pump energy of 480 mJ. The discrepancy of nearly 70 mJ resulted from the different coating characteristics of the OCs. For the plane-parallel cavity, the OC was HR coated at 1.064 μm, enabling double-pass pumping for higher output. While limited by the coating technology, the OC (GRM2) of the unstable cavity was without HR coating for 1.064 μm, and single-pass pumping resulted in lower output energy. To date, this is the highest output level of the OPO with an unstable cavity at 100 Hz PRF. Moreover, the dependence of the output energies on the cavity length is shown in Fig. 4(b)

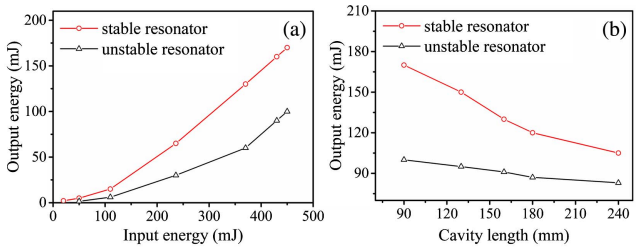

Fig. 4. OPO output pulse energies (sum of signal and idler) for unstable and stable resonators. (a) Output energies versus the incident pump energy at the cavity length of 90 mm. (b) Output energies under different cavity lengths at the pump energy of 480 mJ.

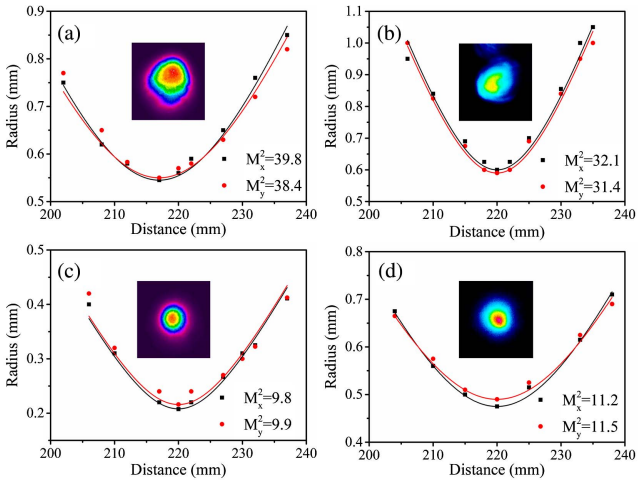

Fig. 5. Beam quality of the signal and idler at the pump energy of 480 mJ. Inset shows the beam profile. (a) Signal of the OPO based on the plane-parallel cavity; (b) idler of the OPO based on the plane-parallel cavity; (c) signal of the OPO based on the unstable cavity with GRM; (d) idler of the OPO based on the unstable cavity with GRM.

under the stable and unstable operation. As the length of the cavity increased, the output energy of both unstable and stable cavities decreases significantly.

To verify that the unstable cavity could improve the beam quality, we obtained the beam profile from a near-infrared CCD (SP620U-MIR, Ophir) and MIR (WinCamD-IR-BB, DataRay) camera. Figure 5 shows the measured beam profiles of the signal and idler, and it was found that both the signal and idler of an unstable cavity had better spatial intensity distribution than those from a stable cavity. At the same pump energy of 480 mJ, the M^2 of the signal and idler in the stable cavity and unstable cavity with GRM were obtained by fitting the beam propagation equation. Figures 5(a) and 5(b) show the beam quality of stable cavity OPO, the M^2 factors of the signal were $M_x^2 = 39.8$ and $M_y^2 = 38.4$, and those of the idler were $M_x^2 = 32.1$ and $M_y^2 = 31.4$. The beam quality of the unstable cavity is shown in Figs. 5(c) and 5(d), the beam quality factors of the signal were about $M_x^2 = 9.8$ and $M_y^2 = 9.9$, and the beam quality factors of the idler were about $M_x^2 = 11.2$ and $M_y^2 = 11.5$. The above results are summarized in Table 1.

A figure of merit that could be used to compare these two works is the brightness. The general definition of a pulsed laser source brightness is given by

Table 1. Beam Quality Values and Output Energy Achieved with the Described Resonators.

	M^2 Factors		Energy (mJ)	
	Stable	Unstable	Stable	Unstable
Signal	39.8/38.4	9.8/9.9	128	75
Idler	32.1/31.4	11.2/11.5	48	26

$$B = \frac{P}{(\lambda M^2)^2}, \tag{9}$$

where λ is the laser wavelength, and P is the laser peak power[44]. According to Figs. 4 and 5, we calculated the brightness of the output laser. The brightnesses of the signal and idler obtained from the unstable cavity with GRM were about 20 GW/(sr · mm^2) and 1.1 GW/(sr · mm^2), respectively, while those obtained from the plane-parallel cavity were 2.2 GW/(sr · mm^2) and 0.26 GW/(sr · mm^2), respectively. The brightnesses of the signal and idler were improved by more than eight times and three times.

Although the beam quality has been greatly improved by using a non-confocal unstable cavity with GRM, the results still need to be further improved. As reported in Ref. [30], the confocal unstable resonator has been shown to be useful for generating beams close to the diffraction limit in the OPO. To realize a confocal unstable resonator with the GRM in hand, the cavity length was increased to satisfy the confocal condition, which resulted in a significant decrease in the OPO efficiency. Building a compact confocal resonator, GRM with a short radius of curvature was required. However, it was difficult for GRMs with short radii of curvature to control damage in a high energy cavity. In future experiments, we will focus on how to use the confocal unstable cavity OPO to obtain high energy laser output with ideal beam quality. We will also improve the beam quality of the 1064 nm pump source to increase the brightness of the OPO's output lasers.

The corresponding output spectral characteristics were measured at a maximum pulse energy of 101 mJ for the unstable cavity with GRM. As shown in Fig. 6, the bandwidth (FWHM) of the signal spectrum was approximately 0.25 nm with a central wavelength of 1535 nm. Based on the phase matching conditions, the idler laser wavelength can be calculated to be 3467 nm.

In addition, an indium gallium arsenide detector, an MIR detector (MIP-10-100M-F-M4, Vigo), and an oscilloscope (Wavesurfer 3034, LeCroy) were used to observe and record the pulse shape of the OPO. The results are shown in Figs. 7(a) and 7(b). At the maximum output energy, the pulse widths of

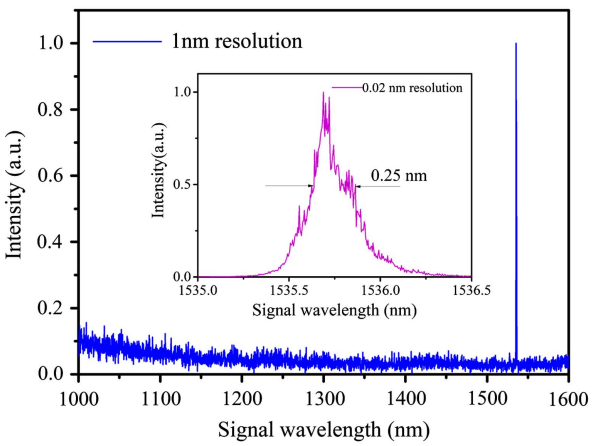

Fig. 6. Spectrum of the signal light.

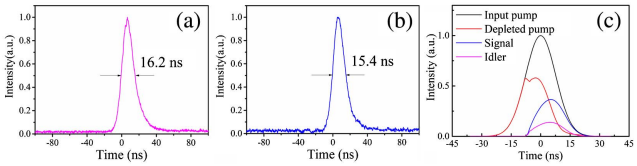

Fig. 7. Typical pulse shapes of OPO based on the unstable cavity with GRM at the output energy of 101 mJ. (a) Temporal profile of the signal in the experiment; (b) temporal profile of the idler in the experiment; (c) the simulation of the temporal profile.

the signal and idler were 16.2 ns and 15.4 ns, respectively. Figure 7(c) shows the simulation of the temporal profile of the depleted pump, signal, and idler pulses. It indicated that the signal and idler pulses build up synchronously when the pump pulse starts the conversion, and the pulse widths were estimated to be 15.6 ns and 15.8 ns for the signal and idler pulses, respectively. In general, these characteristics were basically consistent with the experimental results.

5. Conclusion

In summary, the brightness can be greatly improved by using a GRM and an unstable resonator as compared to the standard plane-parallel resonator. A high beam quality, high energy, unstable cavity KTA-OPO with a PRF of 100 Hz was achieved. The total output energy was about 101 mJ. The beam quality factors of the signal beam at the maximum output energy were about $M_x^2 = 9.8$ and $M_y^2 = 9.9$. The corresponding results of the idler beam were about $M_x^2 = 11.2$ and $M_y^2 = 11.5$. The dual-wavelength high energy OPO system will be a reliable and powerful tool for spectral measurement, remote sensing, and military aspects. Future experiments are devoted to optimizing the magnification of the unstable cavity OPO to optimize the efficiency and divergence of the signal and idler beams while maintaining good beam quality.

Acknowledgement

This work was supported in part by the National Natural Science Foundation of China (Nos. 62075116 and 62075117), Key Research Program of Shandong Province (No. 2019JMRH0111), Natural Science Foundation of Shandong Province (Nos. ZR2019MF039 and ZR2020MF114), Founding for Qilu Young Scholars from Shandong University, and China Postdoctoral Science Foundation (No. 2021TQ0190).

References

1. H. Kong, J. T. Bian, J. Y. Yao, Q. Ye, and X. Q. Sun, "Temperature tuning of $BaGa_4Se_7$ optical parametric oscillator," Chin. Opt. Lett. **19**, 021901 (2021).
2. S. Q. Zha, Y. J. Chen, B. X. Li, Y. F. Lin, W. B. Liao, Y. Q. Zou, C. H. Huang, Z. L. Lin, and G. Zhang, "High-repetition-rate 1.5 μm passively *Q*-switched Er:Yb:$YAl_3(BO_3)_4$ microchip laser," Chin. Opt. Lett. **19**, 071402 (2021).
3. Y. H. Zhu, Z. J. Zheng, X. G. Ge, G. G. Du, S. C. Ruan, C. Y. Guo, P. G. Yan, P. Hua, L. Z. Xia, and Q. T. Lü, "High-power, ultra-broadband supercontinuum source based upon 1/1.5 μm dual-band pumping," Chin. Opt. Lett. **19**, 041403 (2021).
4. D. H. Titterton, "A review of the development of optical countermeasures," Proc. SPIE **5615**, 1 (2004).
5. H. H. P. Th. Bekman, J. C. van den Heuvel, F. J. M. van Putten, and R. Schleijpen, "Development of a mid-infrared laser for study of infrared counter-measures techniques," Proc. SPIE **5615**, 27 (2004).
6. G. A. Rines, D. M. Rines, and P. F. Moulton, "Efficient, high-energy, KTP optical parametric oscillators pumped with 1 micron Nd-lasers," in *Advanced Solid-State Lasers* (Optical Society of America, 1994), p. 461.
7. Y. L. Ju, B. Q. Yao, and S. Qi, "High power 1.57-μm OPO pumped by MOPA with SBS," Chin. Opt. Lett. **3**, 358 (2005).
8. F. F. Wang, J. T. Li, X. H. Sun, B. Z. Yan, H. K. Nie, X. Li, K. J. Yang, B. T. Zhang, and J. L. He, "High-power and high-efficiency 4.3 μm ZGP-OPO," Chin. Opt. Lett. **20**, 011403 (2022).
9. H. Ishizuki and T. Taira, "High energy quasi-phase matched optical parametric oscillation using Mg-doped congruent $LiTaO_3$ crystal," Opt. Express **18**, 253 (2010).
10. G. Y. Liu, S. Y. Mi, K. Yang, D. S. Wei, J. H. Li, B. Q. Yao, C. Yang, T. Y. Dai, X. M. Duan, L. X. Tian, and Y. L. Ju, "161 W middle infrared $ZnGeP_2$ MOPA system pumped by 300 W-class Ho:YAG MOPA system," Opt. Lett. **46**, 82 (2021).
11. J. D. Bierlein, H. Vanherzeele, and A. A. Ballman, "Linear and nonlinear optical properties of flux-grown $KTiOAsO_4$," Appl. Phys. Lett. **54**, 783 (1989).
12. S. Cussat-Blanc, A. Ivanov, D. Lupinski, and E. Freysz, "$KTiOPO_4$, $KTiOAsO_4$, and $KNbO_3$ crystals for mid-infrared femtosecond optical parametric amplifiers: analysis and comparison," Appl. Phys. B **70**, 247 (2000).
13. Q. Liu, Z. L. Zhang, and J. H. Liu, "100 Hz high energy $KTiOAsO_4$ optical parametric oscillator," Infrared Phys. Technol. **61**, 287 (2013).
14. Q. B. Sun, H. J. Liu, N. Huang, C. Ruan, S. L. Zhu, and W. Zhao, "High energy and high efficiency 3.4 μm extra cavity KTA optical parametric oscillator," Laser Phys. Lett. **8**, 16 (2010).
15. Q. Liu, J. H. Liu, Z. L. Zhang, and M. L. Gong, "A high energy 3.75 μm KTA optical parametric oscillator at a critical angle," Laser Phys. Lett. **10**, 075407 (2013).
16. J. C. McCarthy, R. C. Day, and E. Chicklis, "Novel, efficient, high brightness KTP optical parametric oscillator amplifier in single beamline," in *Advanced Solid-State Lasers* (Optical Society of America, 2001), p. 656.
17. J. Liu, Q. Liu, L. Huang, and M Gong, "High energy eye-safe and mid-infrared optical parametric oscillator," Laser Phys. Lett. **7**, 853 (2010).
18. J. Meng, Z. H. Cong, Z. G. Zhao, S. Wang, Y. X. Qi, X. Y. Zhang, and Z. J. Liu, "100 Hz high-energy KTA dual-wavelength optical parametric oscillator," Chin. J. Lasers **48**, 1201009 (2021).
19. A. V. Smith and D. J. Armstrong, "Nanosecond optical parametric oscillator with 90° image rotation: design and performance," J. Opt. Soc. Am. B **19**, 1801 (2002).
20. S. Bigotta, G. Stöppler, J. Schöner, M. Schellhorn, and M. Eichhorn, "Novel non-planar ring cavity for enhanced beam quality in high-pulse-energy optical parametric oscillators," Opt. Mater. Express **4**, 411 (2014).
21. M. A. Medina, M. Piotrowski, M. Schellhorn, F. R. Wagner, A. Berrou, and A. Hildenbrand-Dhollande, "Beam quality and efficiency of ns-pulsed high-power mid-IR ZGP OPOs compared in linear and non-planar ring resonators," Opt. Express **29**, 21727 (2021).
22. D. J. Armstrong and A. V. Smith, "150-mJ 1550-nm KTA OPO with good beam quality and high efficiency," Proc. SPIE **5337**, 71 (2004).
23. A. V. Smith and M. S. Bowers, "Image-rotating cavity designs for improved beam quality in nanosecond optical parametric oscillators," J. Opt. Soc. Am. B **18**, 706 (2001).
24. R. F. Wu, K. S. Lai, H. F. Wong, W. J. Xie, Y. L. Lim, and E. Lau, "Multiwatt mid-IR output from a Nd:YALO laser pumped intracavity KTA OPO," Opt. Express **8**, 694 (2001).
25. S. Pearl, Y. Ehrlich, and S. Fastig, "Optical parametric oscillator with unstable resonators," Proc. SPIE **4972**, 58 (2003).
26. E. V. Raevsky, V. L. Pavlovitch, and V. A. Konovalov, "Efficient eye-safe intracavity KTP optical parametric oscillator," Proc. SPIE **4630**, 75 (2002).
27. W. A. Neuman and S. P. Velsko, "Effect of cavity design on optical parametric oscillator performance," in *Advanced Solid-State Lasers* (Optical Society of America, 1996), p. 179.

28. S. S. Zou, M. L. Gong, Q. Liu, and G. Chen, "Low threshold characteristic of pulsed confocal unstable optical parametric oscillators with Gaussian reflectivity mirrors," Opt. Express **13**, 776 (2005).
29. M. K. Brown and M. S. Bowers, "High energy, near diffraction limited output from optical parametric oscillators using unstable resonators," Proc. SPIE **2986**, 113 (1997).
30. B. C. Johnson, V. J. Newell, J. B. Clark, and E. S. Mcphee, "Narrow-bandwidth low-divergence optical parametric oscillator for nonlinear frequency-conversion applications," J. Opt. Soc. Am. B **12**, 2122 (1995).
31. J. N. Farmer, M. S. Bowers, and W. S. Schaprf, Jr., "High brightness eye safe optical parametric oscillator using confocal unstable resonators," in *Advanced Solid-State Lasers* (Optical Society of America, 1999), p. 567.
32. W. Scharpf, G. Ferguson, B. Boczar, M. S. Bowers, and M. K. Brown, "An eye safe KTA OPO with an unstable resonator," in *Advanced Solid-State Lasers* (Optical Society of America, 1998), p. 189.
33. G. Hansson, H. Karlsson, and F. Laurell, "Unstable resonator optical parametric oscillator based on quasi-phase-matched $RbTiOAsO_4$," Appl. Opt. **40**, 5446 (2001).
34. A. I. Vodchits, V. I. Dashkevich, N. S. Kazak, V. K. Pavlenko, V. I. Pokryshkin, I. P. Petrovich, V. V. Rukhovets, A. S. Kraskovskii, and V. A. Orlovich, "Eye-safe radiation source based on an optical parametric oscillator," J. Appl. Spectrosc. **73**, 285 (2006).
35. M. Morin, "Graded reflectivity mirror unstable laser resonators," Opt. Quantum Electron **29**, 819 (1997).
36. M. Morin and M. Poirier, "Graded reflectivity mirror unstable laser resonator design," Proc. SPIE **3267**, 52 (1998).
37. K. J. Snell, N. Mccarthy, and M. Piché, "Single transverse mode oscillation from an unstable resonator Nd:YAG laser using a variable reflectivity mirror," Opt. Commun. **65**, 377 (1988).
38. S. Chandra, T. H. Allik, J. A. Hutchinson, and M. S. Bowers, "Improved OPO brightness with a GRM non-confocal unstable resonator," in *Advanced Solid-State Lasers* (Optical Society of America, 1996), p. 177.
39. S. Zou, M. Gong, P. Yan, G. Chen, and Q. Liu, "Buildup time of pulsed confocal unstable optical parametric oscillator," in *Advanced Solid-State Photonics (TOPS)* (Optical Society of America, 2005), p. 391.
40. A. V. Smith, *Crystal Nonlinear Optics: With SNLO Examples* (AS-Photonics, 2018).
41. P. B. Phua, R. F. Wu, and T. C. Chong, "Nanosecond MIR $AgGaS_2$ OPO and its numerical modelling," in *Advanced Solid State Lasers* (Optica Publishing Group, 1998), paper FC14.
42. A. V. Smith, W. J. Alford, T. D. Raymond, and M. S. Bowers, "Comparison of a numerical model with measured performance of a seeded, nanosecond KTP optical parametric oscillator," J. Opt. Soc. Am. B **12**, 2253 (1995).
43. Z. Sacks, O. Gayer, E. Tal, and A. Arie, "Improving the efficiency of an optical parametric oscillator by tailoring the pump pulse shape," Opt. Express **18**, 12669 (2010).
44. T. Kawasaki, V. Yahia, and T. Taira, "100 Hz operation in 10 PW/sr·cm^2 class Nd:YAG Micro-MOPA," Opt. Express **27**, 19555 (2019).